JOURNAL OF GEOPHYSICAL RESEARCH, VOL. 101, NO. D21, PAGES 26,517–26,525, NOVEMBER 27, 1996

Hydrological applications of satellite data 1. Rainfall estimation

A. A. Tsonis and G. N. Triantafyllou [1]

Department of Geosciences, University of Wisconsin–Milwaukee

K. P. Georgakakos [2]

Hydrologic Research Center, San Diego, California

Abstract. In this study we investigate the ability of satellite visible and infrared data to produce reliable rainfall amount estimates that could be used by hydrological models to predict streamflow for large basins. Rainfall estimates are obtained by (1) classification of clouds to raining and nonraining clouds and (2) applying a multivariate statistical model between rainfall and indices derived from the satellite observations. Satellite data corresponding to 180 randomly selected days in the period May–September 1982–1988 are used in this study that focuses on the estimation of daily rainfall. The Des Moines River basin in the midwestern United States is the application area. The correlation coefficient between model-predicted and rain gauge-observed mean areal precipitation over areas of order 10,000 km^2 is found to be about 0.85. In an example application the satellite rainfall estimates are used to force the operational National Weather Service hydrologic forecast model for a subbasin of the Des Moines River basin. The model has been calibrated with rain gauge data. The results show that differences between rain gauge and satellite rainfall input generate differences in flow forecasts and upper soil water model estimates, which are a function of the antecedent soil water conditions. A companion paper [*Guetter et al.*, this issue] quantifies the effects that the differences between rain gauge and satellite rainfall estimates have on flow and upper soil water model predictions for various spatial scales and for hydrologic models calibrated with and without satellite data.

1. Introduction

Real-time flow prediction in large catchments has seen significant advances in the last few decades mainly as a result of the following two reasons: (1) the use of the computer with numerical hydrological models has facilitated computations associated with the discretization of large catchments to smaller hydrologic units and has allowed the utilization of complex hydrologic and hydraulic simulation models in real time, and (2) advances in sensor and communication technology allowed the use of real-time hydrometeorologic data obtained at remote sites. Thus conceptual hydrologic models are routinely used in the United States for the real-time prediction of streamflow from headwater basins [e.g., *Peck,* 1976; *Brazil,* 1989; *Georgakakos,* 1986a, b]. Similarly, hydraulic river routing models have been used in the real time simulation and prediction of flow in large rivers [e.g., *Fread,* 1985]. Automated real-time databases that include data from automated on-site sensors are becoming the norm for Federal and State Agencies with real-time flow prediction and water resource management missions [e.g., *Bae et al.,* 1995; *Georgakakos and Smith,* 1990; *HRL Staff,* 1972].

Real-time flow prediction along those lines was based on the determination of mean areal rainfall estimates from point rainfall data. In recent years the digitization of radar reflectivity data and their conversion to rainfall estimates has prompted the development of models suitable to accept input that is spatially distributed in small spatial scales (e.g., see articles in the works of *Collinge and Kirby* [1987] and *Wyss et al.* [1990]). Also, methods for merging radar rainfall data with rain gauge data have been developed for a more reliable estimation of mean areal rainfall over hydrologic catchment units [e.g., *Creutin and Obled,* 1982; *Krajewski,* 1987].

Here we extend the above effort by examining the feasibility of using physically based hydrologic and hydraulic models driven by mean areal rainfall estimates obtained from satellite (GOES) visible (VIS) and infrared (IR) temperature data. This problem is of par-

[1] Now at Institute of Marine Biology of Crete, Iraklio, Crete, Greece.

[2] Also at Scripps Institution of Oceanography, La Jolla, California.

Paper number 96JD01654.
0148-0227/96/96JD-01654$09.00

ticular interest for situations where other rainfall input is lacking or is unreliable (remote areas, mountainous terrain, etc). The presentation is divided in two parts. This paper presents the rainfall estimation procedure from satellite visible and infrared data and shows examples of application of the estimated rainfall to predict river flows. The second part [*Guetter et al.,* this issue] is a more detailed analysis of the utility of satellite data in operational hydrologic forecasting on various spatial scales.

2. Rainfall Estimation From Satellite Imagery

2.1. Related Work

In order to derive a mean rainfall amount for a given area we must first produce the rain area from the satellite images, and then we should link this estimate to rain amounts on the ground. In the past many methods to delineate rain area form satellite images have been proposed. Those techniques can be divided into three major categories: (1) the indexing techniques, (2) the life history techniques, and (3) the bispectral methods. According to the indexing techniques (for a review, see *Barrett and Martin* [1981]), rainfall depends on the cloud type. The rainfall area is found after the clouds have been classified to various types according to their spectral properties. The life history methods make use of information provided by the last two preceding half-hour GOES infrared images in order to estimate point rainfall rates [*Scofield and Oliver,* 1977; *Griffith et al.,* 1978] and volumetric rain rates [*Stout et al.,* 1979]. These techniques are based on the observed growth of the clouds (which are defined by a single visible or infrared threshold) and have provided very useful results especially in cases of strong convection. According to the bispectral methods the rain area is determined using information from both visible and IR images [*Lovejoy and Austin,* 1979; *Bellon et al.,* 1980]. Basically, these techniques define an optimum boundary in the visible/infrared domain which is used to discriminate between rain and no-rain. This optimum boundary is defined using an original pattern recognition technique involving satellite and coextensive radar data. According to this technique the probability of precipitation as a function of VIS and IR intensity is found, and then an appropriate probability threshold is determined that delineates a satellite rain area equal to the observed radar rain area. Since the probability of precipitation is different from day to day, these methods depend on radar data, and therefore their applicability is limited to only areas over which adequate coverage is available. Subsequently, *Tsonis and Isaac* [1985] developed a technique in which the optimum boundary is determined without the need of coextensive radar data; radar data are used only for training and verification purposes. Their technique makes use of the bivariate frequency distribution in the visible/infrared domain. It has been shown [*Tsonis,* 1984] that the observed peaks of such distribution correspond to different classes. *Tsonis and Isaac* [1985] showed that the peaks that correspond to raining clouds tend to cluster in a well-defined region of the visible/infrared domain thus allowing their discrimination from the other classes (clear skies, nonraining clouds, etc.). After a peak has been attributed to raining clouds the rain area is defined via a simple stepwise procedure outlined by *Tsonis and Isaac* [1985].

Most if not all, however, of the above approaches have no success in providing information on mean area rain rate. This is explicitly investigated by *Negri et al.*[1984] and *Negri and Adler* [1987a, b]. It is demonstrated (for convective cases, only) that while the satellite data are quite promising in delineating rain area, they are not adequate in providing any mean-area rain rate information.

Thus, after the rain area has been estimated from the VIS/IR satellite data we must look somewhere else if we wish to assign an average rain rate (and consequently total rain amounts) for that area. A first answer to this problem has been recently proposed by *Rosenfeld et al.* [1990]. According to them, instantaneous area average rain rate R can be obtained with $5-10\%$ accuracy over a large domain by measuring the fraction of the total radar rain area $F_r(\tau)$ covered by rain intensity greater than a threshold τ. For each radar scan, $F_r(\tau)$ together with R are found, and the corresponding point is plotted on a R versus $F_r(\tau)$ diagram. Accumulating many such data points allowed Rosenfeld et al. to obtain fairly accurate relations between R and $F_r(\tau)$. They have demonstrated that $R = f(F_r(\tau))$, where f is linear. Thus, if for a given area we derive the function f (which most likely varies with climatology), we can estimate a mean rain rate for the area. It is interesting to note here that the existence of those relationships has actually been predicted theoretically [*Atlas et al.,* 1990; *Kedem et al.,* 1990]. In the work of Kedem et al., for example, the precise linear relationship between the area average rain rate and fractional area covered by rain above a fixed threshold is theoretically highlighted by observing that rain rate has a certain mixed distribution. Of course, in our case we do not have the rain area from a weather radar but from satellite data. Note that the rain area derived from satellite imagery is not the cloud area. Such rain area approximates the actual area whose boundary is the 0.0 mm/h isopleth. Thus, if the above approach is employed in our study, we will have to assume that the satellite-derived rain area is the actual rain area for $\tau = 0.0$ mm/h. We will denote this fraction as $F_s(0)$, where the subscript s stands for satellite. Thus we will be seeking a relation between $F_s(0)$ and R averaged over a proper time interval. In this study we will adopt as this time interval the length of a day (24 hours). This interval is based on considerations of basin response and on tests of the employed hydrologic/hydraulic model with historical data.

2.2. Study Area and Data

The Des Moines River basin with outlet at Stratford (Figure 1) is an ideal test area since an extensive

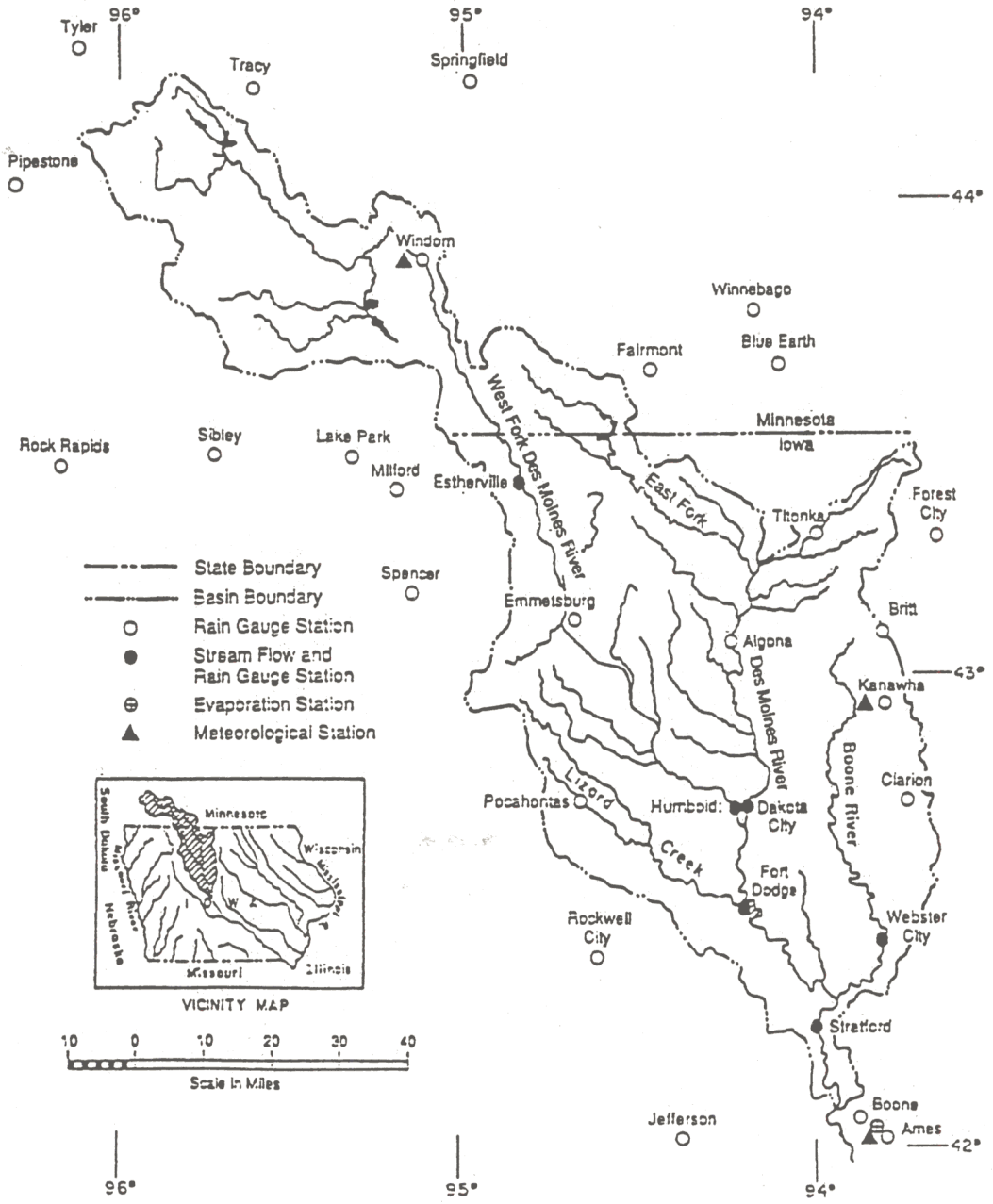

Figure 1. The geographical area of interest.

and prototype real-time hydrometeorological database (a network of 29 rain gauges and 2 radars) exists for that area as part of the U.S. Corps of Engineers, Rock Island District real-time monitoring system. Also, several hydrologic models (i.e., an API model, the HEC1 model, and the modified Sacramento model) have been implemented and are now in operational use for predicting flows in the aforementioned 15,000 km^2 basin [e.g., *Bae et al.*, 1995; *Bae and Georgakakos*, 1994]. The dense rain gauge network provides hourly amounts of precipitation in the area of interest. Daily mean areal rainfall amounts are computed for the whole basin according to the standard National Weather Service (NWS) interpolation procedures.

The satellite data used in this work are GOES visible (0.54–0.70 μm) wavelength and infrared (10.5–12.6 μm) wavelength images. The temporal resolution of the satellite data is 30 min, and the spatial resolution is 4×4 km. It should be noted at this point that the resolution of the sensed infrared images is 4×8 km. From these images, 4×4-km-resolution images are usually constructed for a better resolution equivalence between the infrared and visible data. The intensity (count) range of the visible and infrared images is 0–255.

The satellite data are used to develop a scheme that will delineate the rain area over the region of interest. The scheme of *Tsonis and Isaac* [1985] will be applied to define the boundaries (in VIS/IR space) that separate

rain from no-rain. In order to derive those boundaries (climatology) we considered the period May–September 1982–1988 and selected images every 3 hours from 180 randomly selected days. Sampling every 3 hours guarantees that successive images will not be correlated [*Tsonis and Isaac,* 1985]. From those days a training sample of 175 days were used to derive the climatology, and the remaining 5 days were used for verification. Because the visible images will be involved in the analysis, only VIS/IR pairs at 1200, 1500, 1800 and 2100 Local Time (LT) can be considered. Thus, for a given day, satellite statistics are based on, at most, four VIS/IR pairs or on information for at most 12 hours. Since the area of interest is about 208×336 km^2, the VIS/IR images (at a resolution of 4×4 km^2) provide over 6,000,000 pixel values for the entire area. This is more than enough to ensure an accurate determination of the satellite climatology of the area. For the same times we also decided to use the daily rainfall amounts derived from the available dense rain gauge network. This data set will help in the discrimination of the raining and nonraining clouds that is necessary for the Tsonis and Isaac approach and to derive the relationship between the rain area which will then be used by the hydrological models. We chose the rain gauge data in favor of radar data because (1) the entire area is not covered by a single radar (this introduces problems in the overlapping region due to different radar calibrations), (2) we are interested in total amounts on the ground rather than actual rain area and intensity at a specific level, and (3) the rain gauge system is as effective as a radar in applying the Tsonis–Isaac procedure.

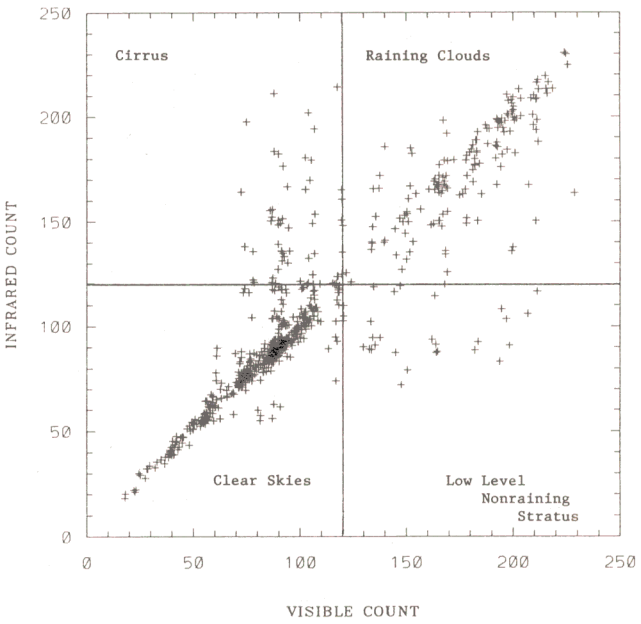

Figure 2. Location of the peaks resulting from bivariate distributions in the visible/infrared (VIS/IR) domain. The peaks in the bottom left correspond to clear skies, peaks in the bottom right correspond to low-level nonraining clouds and fog, peaks in the top left correspond to high-level nonraining clouds (cirrus), and peaks in the top right correspond to raining clouds. Data are based on satellite images from 180 randomly selected days.

2.3. Procedure and Results

Using the training sample, for each one of the available times and for every available VIS/IR pair of images, the bivariate frequency distribution was derived over the area of interest by subdividing the data into intervals of 16 units wide in both the visible and infrared domain. We will denote this frequency as $f(i,j)$ $i,j = 1,16$. If the resulting frequency at any of the 16×16 entries is greater than the immediate eight neighbor entries, that indicates a peak and the corresponding frequency is denoted as $f(i_p, j_p)$. The exact coordinates in the VIS/IR domain of the peak (V_p, I_p) are then determined by considering the weight of each one of its neighbors. Figure 2 shows the location of all the peaks in the VIS/IR domain. In order to avoid contamination of Figure 2 due to small-scale and/or spurious peaks, only peaks that correspond to at least a relative frequency of 0.05 were considered. This plot is very similar to the one initially produced by *Tsonis and Isaac* [1985] but it includes 1 order of magnitude more data. The plot can roughly be divided into four quarters by straight lines VIS=120 and IR=120 that would separate the following main classes: Bottom left quarter, clear skies; bottom right quarter, low-level nonraining stratus clouds; top left quarter, cirrus clouds; and top right quarter, raining clouds.

The accuracy of the scheme in predicting rainy days is approximately 88%. This estimate is derived as follows: If one or more VIS/IR pairs results in bivariate distributions with peaks that are attributed (from Figure 2) to raining clouds, then the day is classified as a rainy day. Seventy-seven days in our training sample are classified as rainy days. The classification is considered as accurate if the daily average rainfall amount from the rain gauge network is greater than 0.025 inches/d (0.064 cm/d). Accordingly, we find that 68 of the 77 days ($\approx$ 88%) were correctly classified as rainy days. The accuracy of the scheme in predicting nonraining days is about 92%. Now the scheme classifies a day as nonrainy if all four VIS/IR pairs produce bivariate distributions which show no peaks attributed to raining clouds. Sixty-four days in our training sample were thus classified as nonrainy. Here a classification is considered as accurate if the daily average rainfall amount for the rain gauge network is less than 0.025 inches/d (0.064 cm/d). Accordingly, we find that 59 out of the 64 days ($\approx$ 92%) are correctly classified as nonrainy days. Days for which the above conditions were not met were not classified and were not considered in the following calculations. This critical value of 0.025 inches/d (0.064 cm/d) was chosen in order to avoid contamination of the statistics from small scales or random events.

In the work of *Tsonis and Isaac* [1985], once a peak has been assigned to raining clouds the rain area is determined from all pixels having a visible count greater or equal to V_p. This area would be an estimation of $F_s(0)$. Having established the above, the first task was to determine whether or not the derived $F_s(0)$ will pro-

duce a daily average $\overline{F}_s(0)$ that is well correlated to the daily mean areal rainfall $\overline{R}$. The average $\overline{F}_s(0)$ is obtained from the pairs of visible and infrared images available for that day. The procedure is subject to the following errors. If most of the rain falls at night, satellite estimates of rainfall amounts would be too small. If most of the rain falls during the day, satellite estimates would be close to actual rainfall amounts as long as sufficient information (i.e., VIS/IR pairs) is available. If there is insufficient information, satellite estimates can be either smaller or larger than actual rainfall amounts.

In Figure 3 it is concluded that $\overline{F}_s(0)$ is actually uncorrelated to $\overline{R}$. Note that lately *Short et al.*, [1993] have demonstrated good correlations between $\overline{R}$ and $\overline{F}_r(0)$, where $\overline{F}_r(0)$ is defined from continuous radar coverage and $\overline{R}$ is defined from a rain gauge network. Thus, if a similar relation exists between $\overline{F}_s(0)$ and $\overline{R}$, the source of the above errors has to be minimized. A possible remedy would be to consider days for which satellite coverage is as large as possible. Given the limitations of the visible images, we decided to eliminate all raining days for which we did not have at least three VIS/IR pairs available. That left us with 24 raining days in our training sample and 3 in our verifying sample. Figure 4 shows $\overline{F}_s(0)$ versus $\overline{R}$ for those 24 days. We now see that the relation becomes a bit clearer. The coefficient of determination r^2 of a linear fit of $\overline{F}_s(0)$ on $\overline{R}$ is ≈ 0.45. This means that that $\overline{F}_s(0)$ explains $\approx 45\%$ of the variance of $\overline{R}$. We deem this as not quite acceptable for our purposes. We therefore decided to look for more variables that could be considered in the problem of estimating a daily average rainfall amount from satellite VIS/IR images.

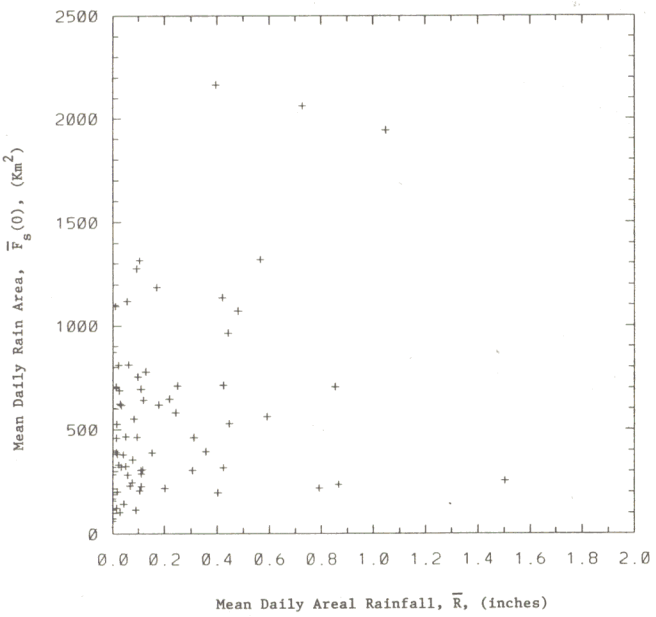

Figure 3. For a given pair of VIS/IR images, if a peak in the bivariate distribution is attributed to raining clouds, a rain area according to *Tsonis and Isaac* [1985] is produced. From all the available pairs in a given day the average area is estimated and is plotted against the daily area-averaged amount of rain on the ground as given from a network of 29 rain gauges. A good relationship does not emerge. Part of the problem is due to the fact that VIS/IR pairs were not available throughout the day, and rain often fell when satellite data were not available.

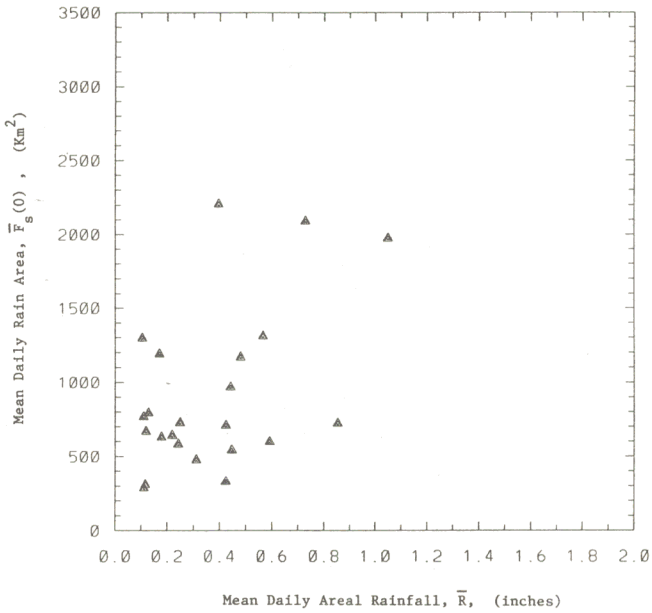

Figure 4. Same as Figure 3, but including days for which at least three VIS/IR pairs are available. A better relationship begins to emerge, but the overall coefficient of determination is 0.45. We consider this result as unsatisfactory, and we continue with the development of a multivariate model.

2.4. A Multivariate Model

In searching for other satellite variables that would increase the correlation between predicted and actual rain amount we turn again our attention to the bivariate distribution. Figure 5 shows bivariate distributions for June 14, 1983 at 1500 LT (Figure 5a) and August 26, 1987 at 1500 LT (Figure 5b). Figure 5a exhibits two not very pronounced and rather wide peaks. The peak at high-visible and high-infrared counts corresponds to raining clouds. The other corresponds to clear skies. Figure 5b exhibits a peak which is very pronounced and very narrow and corresponds to raining clouds. The corresponding rainfall amount in the latter case is greater than that in the former case.

Investigation of many bivariate distributions pointed out that, on the average, for peaks that correspond to raining clouds greater rainfall amounts tend to correspond to (1) narrower peaks, (2) higher frequencies of the peak, $f(i_p, j_p)$, and (3) larger coordinates of the peak in the VIS/IR domain, V_p and I_p. We also found that the mean visible count for the cloud area delineated from all pixels with a visible count $V > V_c$ (the subscript c corresponds to the visible count that separates clouds from no-clouds) is often useful (see also *Negri and Adler* [1987a, b]). According to *Tsonis* [1984], $V_c \approx 120$. We will denote this mean visible count as $< V >$. The above statistics are expected to relate to physics underlying the problem. Large $< V >$, V_p, and I_p values

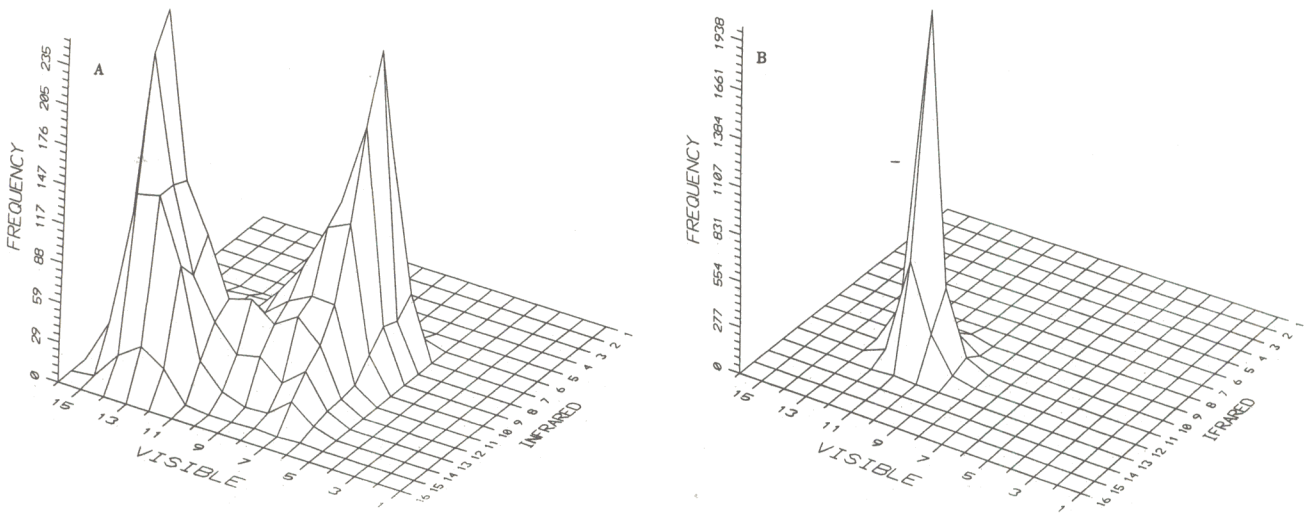

Figure 5. Bivariate distribution for (a) June 14, 1983 at 1500 local time (LT) and (b) August 26, 1987 also at 1500 LT. As is explained in the text, the general shape of these distributions provides clues for improved rain estimation.

indicate thicker and taller clouds, and large $f(i_p, j_p)$ together with a narrow peak indicate that thicker and taller clouds dominate the area. In such cases, more rainfall is anticipated. Note that the employed variables define the shape and location of a peak attributed to raining clouds and thus characterize the "satellite" rainfield to a large degree. We thus decided to build a six-variable multivariate model of the form

$$\begin{aligned} \overline{R} &= a_1\overline{F}_s(0) + a_2\overline{f}(i_p, j_p) + a_3\overline{V}_p \\ &\quad + a_4\overline{I}_p + a_5\overline{S}_{V,I} + a_6 < \overline{V} > \end{aligned} \tag{1}$$

where the bar indicates daily average, R (inches per day) is the area-averaged rainfall amount, $F_s(0)$ is the rain area (km^2) as delineated by the previously described approach, $f(i_p, j_p)$ is the relative frequency of the peak, V_p and I_p are the coordinates of the peak in VIS/IR domain, $< V >$ is the mean visible count of the cloud area, and $S_{V,I}$ is the measure of the narrowness of the peak, which is defined as

$$S^2_{V,I} = \frac{1}{9}\sum_{k=i_p-1}^{i_p+1}\sum_{l=j_p-1}^{j_p+1}(f(k,l) - \overline{f})^2 \tag{2}$$

where

$$\overline{f} = \frac{1}{9}\sum_{k=i_p-1}^{i_p+1}\sum_{l=j_p-1}^{j_p+1} f(k,l) \tag{3}$$

For our raining training sample, (n = 24) we found that $a_1 = -4.987 \times 10^{-6}$, $a_2 = 2.842$, $a_3 = -1.387 \times 10^{-2}$, $a_4 = -2.943 \times 10^{-3}$, $a_5 = -1.335 \times 10^{-3}$, and $a_6 = 1.89 \times 10^{-2}$.

The above statistical model results in a multiple regression coefficient of determination $r^2 = 0.70$ (i.e., $r \approx 0.84$). Variations of this model (to include a nonzero intercept and/or fewer variables) were also considered but resulted in smaller r^2 values. Our six variables explain 70% of the variance of $\overline{R}$ as measured by the rain gauge network. More specifically, we find that $\overline{F}_s(0)$, $\overline{f}(i_p, j_p)$, $\overline{V}_p$, $\overline{I}_p$, $\overline{S}_{V,I}$, and $< \overline{V} >$ explain 46%, 6%, 3%, 2%, 9%, and 4%, respectively of the variance in $\overline{R}$. We consider this result a great improvement over satellite-derived rain area alone. Note that eliminating any of the six variables results in smaller r^2 values.

Subsequently, we applied the overall procedure and statistical model to the 5 remaining days in the training sample. Out of those 5, 3 were correctly classified

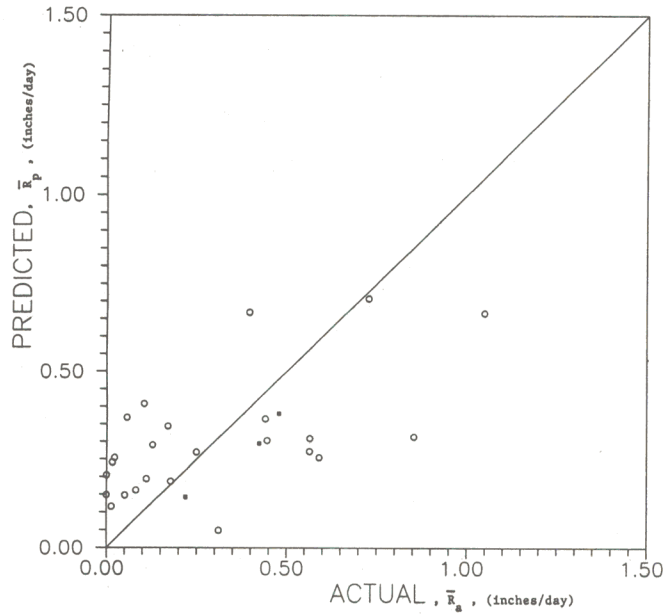

Figure 6. Predicted from the multivariate model, daily area-averaged rain amount versus the actual amount for the training sample (open circles) and the verifying sample (black squares). The overall coefficient of determination is now 0.70.

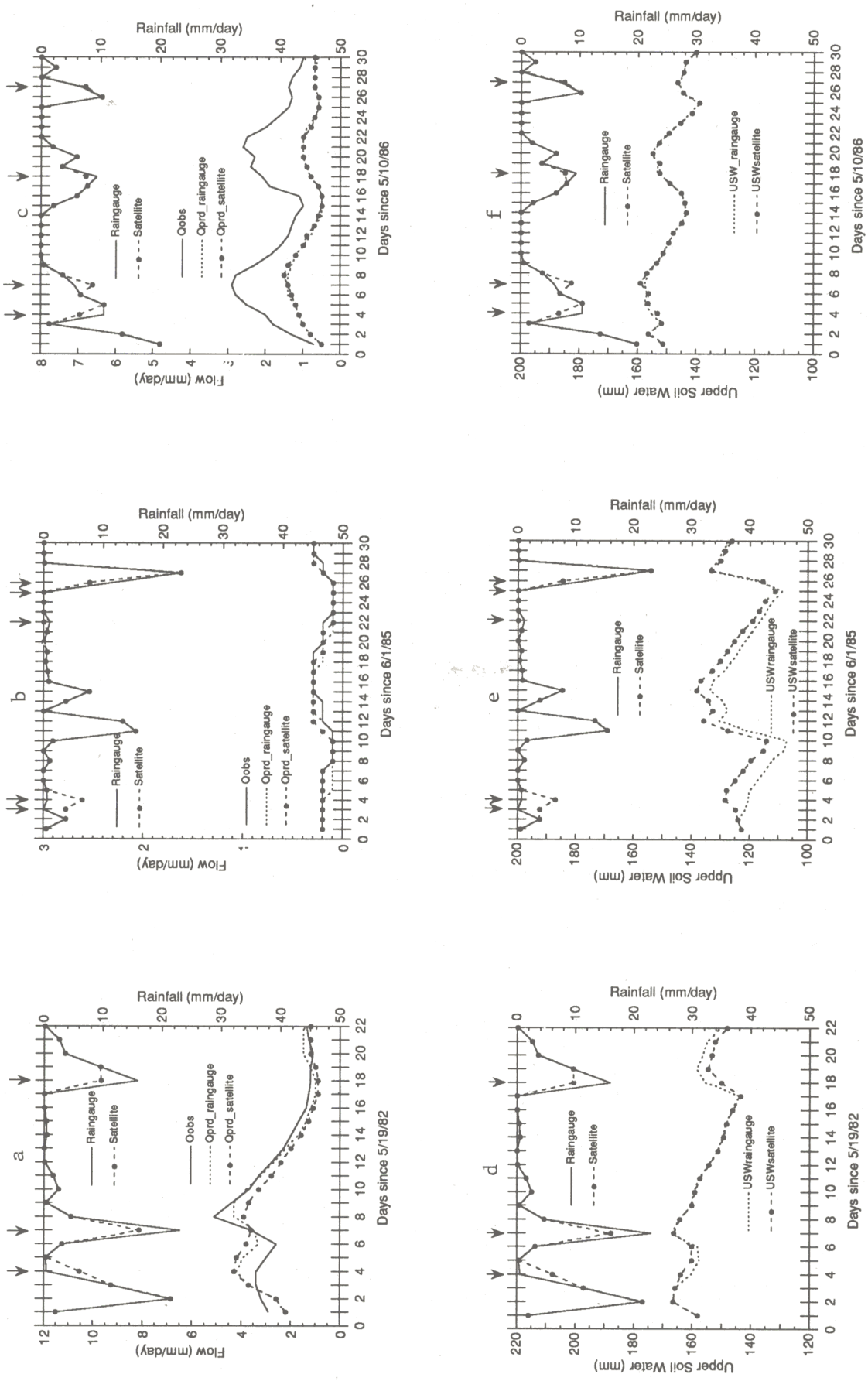

Figure 7. Daily river flows and upper soil water estimates by the hydrologic model, forced by rain gauge and satellite rainfall for three periods: May 19, 1982 to June 10, 1982, June 1, 1985 to June 30, 1985, and May 10, 1986 to June 10, 1986. (a)–(c) Flow and (d)–(f) upper soil water. In both cases rainfall is inverted on the horizontal axis and it is read on the right vertical axis. Satellite-forced cases are shown with dashed line and solid circles. Arrows on the top indicate times when satellite data were available.

as rainy days (June 6, 1982; May 24, 1984; and May 27, 1986). The remaining 2 (August 8, 1983, and July 7, 1985) were correctly classified as nonrainy days. For the 3 rainy days the rain gauge network reported area average daily rainfall of 0.479, 0.219, and 0.424 inches/d, respectively. Equation (1) predicts 0.380, 0.143, and 0.295 inches/d, respectively. Figure 6 shows for the available data the predicted, $\overline{R_R}$ versus the actual, $\overline{R_a}$ using equation (1). Note that a cross-validation procedure results in very comparable results. The parameter values of the multivariate model may differ somewhat, but the general conclusions remain similar. This suggests that multivariate regression models and the variables chosen have captured the essence of the problem and can provide acceptable rainfall estimates. Thus they show promise for further use in studies in the area of rainfall estimation from satellite data.

2.5. Examples of Hydrologic Forecasts

The Sacramento soil water accounting model used in operational hydrologic forecasting by the U.S. National Weather Service [*Bae and Georgakakos*, 1994] and a kinematic routing procedure [*Georgakakos and Bras*, 1982] were used to forecast daily flows in the 2160 km^2 Boone River subbasin of the Des Moines River basin. The Boone River basin with outlet at Webster City, Iowa, is located in the easternmost portion of the Des Moines River basin. *Bae and Georgakakos* [1994] and *Georgakakos et al* [1995] describe the basin hydrology and the calibration and validation of the hydrologic model with rain gauge rainfall data. Cross correlations between the daily observed and predicted flows were about 0.85 with a ratio of residual mean to observed flow mean of 0.02.

Two experiments were made with the available satellite estimates of rainfall. The hydrologic model was run twice for the period from January 1, 1980, through December 31, 1987. The first time the rain gauge data comprised the forcing of the hydrologic model. The second time the satellite data were used when available. During the second run, when satellite data were not available (most of the time), rain gauge rainfall was used. Satellite rainfall estimates corresponding to the large Des Moines River basin area were used as input for the smaller Boone River basin in this preliminary study. The companion paper [*Guetter et al.*, this issue] examines the problem of spatial scale in detail.

Figure 7 shows the following three time periods: a period of high flows well predicted by the calibrated model, a period of low flows well predicted by the calibrated model, and a period of average flows underestimated by the calibrated model. In Figures 7a-7c the observed and predicted Boone River basin flows at Webster City, Iowa, are shown for the cases of rain gauge and satellite rainfall. Inverted on the horizontal axis are the rainfall estimates with arrows indicating the times for which we had satellite data. Figures 7d-7f show upper soil water estimates of the Sacramento model for each case together with inverted rainfall on the horizontal axis. It is apparent that the satellite rainfall estimates are reasonable. During the first period when upper soil water is near saturation, an increased satellite rainfall amount generates an overprediction in upper soil water, which in turn generates a noticeable overprediction of the flow around day 5 from start. On the other hand, substantial overprediction of the upper soil water during the first part of the second period results in a minor overprediction of the satellite-driven flow as compared to the flow forced by rain gauge rainfall. These results indicate that the effect of differences between satellite and rain gauge rainfall estimates on flow predictions depends on antecedent soil water conditions. The results for the third period corroborate this observation and in addition show that calibration problems with the operational hydraulic models will likely persist when satellite rainfall data are used.

These results indicate that quantifying the effects of differences between satellite and rain gauge rainfall on hydrologic forecasts must involve a comprehensive study that covers the full dynamic range of response of the models. In addition, it should account for the issue of model calibration using the satellite data versus using only the rain gauge rainfall data. Such a study is described in paper by *Guetter et al.* [this issue].

3. Comments and Concluding Remarks

In this study we investigated the feasibility of estimating areal averages of rain amounts from satellite VIS/IR imagery. We presented an approach by which these amounts can be obtained using information extracted from bivariate distributions and a multivariate model. Our approach requires the use of visible images. As such, it relies on information during the daytime only. Accordingly, as discussed earlier, our approach would result in errors if precipitation falls at night. Considering the diurnal variations of rainfall in this region [*Wallace*, 1975; *Winkler et al.*, 1988], errors are quite likely. Refinements must be considered before such an approach becomes operational. Possible improvement may result from using only IR images during the nighttime. Research in this area is in progress, and results will be reported later. Nevertheless, even with this limitation, we show that our methodology has the potential for producing acceptable estimates of areal averages of rain amounts. As *Guetter at al.* [this issue] reports, these estimates can effectively be used as input to hydrological models for streamflow prediction and soil moisture estimation.

Acknowledgments. This work was supported by NSF grant BCS–9207943 to A.A.T. and by NSF grant BCS–9496278 to K.P.G.

References

Atlas, D., D. Rosenfeld, and D.A. Short, The estimation of convective rainfall by area integrals, 1, The theoretical and empirical basis, *J. Geophys. Res.95*, 2153–2160, 1990.

Bae, D.H., and K.P. Georgakakos, Climatic variability of soil water in the American Midwest, 1, Hydrologic modeling, *J. Hydrol., 162*, 355–377, 1994.

Bae, D.H., K.P. Georgakakos, and S.K. Nandba,Operational forecasting with real-time databases, *J. Hydraul. Eng., 121*, 49–60, 1995.

Barrett, E.C., and D.W. Martin, *The Use of Satellite Data in Rainfall Monitoring*, 340pp, Academic, San Diego, Calif., 1981.

Bellon, A., S. Lovejoy, and G.L. Austin, Combining satellite and radar data for the short range forecasting of precipitation, *Mon. Weather Rev., 108*, 1554–1566, 1980.

Brazil, L., Multilevel calibration strategy for complex hydrologic simulation models, *NOAA Tech. Rep. NWS 42*, 178pp, Natl. Oceanic and Atmos. Admin., Silver Spring, 1989.

Collinge, V., and C. Kirby (Eds.), *Weather Radar and Flood Forecasting*, 296 pp, John Wiley, New York, 1987.

Creutin, J.D., and C. Obled, Objective analysis and mapping techniques for rainfall fields: An objective comparison, *Water Resour. Res., 18*(2), 413–431, 1982.

Fread, D.L., Channel routing, in *Hydrological Forecasting*, edited by M.G. Anderson and T.P. Burt, pp. 437–503, John Wiley, New York, 1985.

Georgakakos, K.P., A generalized stochastic hydrometeorological model for flood and flash-flood forecasting, 1, Formulation, *Water Resour. Res., 22*(13), 2083–2095, 1986a.

Georgakakos, K.P., A generalized stochastic hydrometeorological model for flood and flash-flood forecasting, 2, Case studies, *Water Resour. Res., 22*(13), 2096–2106, 1986b.

Georgakakos, K.P., and R.L. Bras, Real-time, Statistically linearized adaptive flood routine, *Water Resour. Res., 18*, 513–524, 1982.

Georgakakos, K.P., and G.F. Smith, On improved operational hydrologic forecasting: Results from a WMO real-time forecasting experiment, *J. Hydrol., 114*, 17–45, 1990.

Georgakakos, K.P., D.H. Bae, M.G. Mullusky, and A.P. Georgakakos, Hydrologic variability in midwestern drainage basins: Diagnosis, prediction and control, in *Proceedings of the Symposium on Global Change II, A Midwest Perspective*, edited by E. Folk, chap. II.2, pp. 19–60, SPB Academic, The Hague, Netherlands, 1995.

Griffith, G., W.L. Woodley, P.G. Grube, D.W. Martin, J.Stout, and D.N. Sikdar, Rain estimation from geosynchronous satellite imagery - visible and infrared studies, *Mon. Weather Rev., 106*, 1153–1171, 1987.

Guetter, A.K., K.P. Georgakakos, and A.A. Tsonis, Hydrologic applications of satellite data, 2, Flow simulation and soil water estimates, *J. Geophys. Res.*, this issue.

HRL Staff, National Weather Service river forecast procedures, *NOAA Tech. Memo. NWS HYDRO-14*, Natl. Oceanic and Atmos. Admin., Silver Spring, Md, 1972.

Kedem, B., L.S. Chiu, and G.R. North, Estimation of mean rain rate: Application to satellite observations, *J. Geophys. Res., 95*, 1965–1972, 1990.

Krajewski, W.F., Co-kriging radar-rainfall and raingauge data, *J. Geophys. Res., 92*(D8), 9571–9580, 1987.

Lovejoy, S., and G.L. Austin, The delineation of rain areas from visible and IR satellite data for GATE and midlatitudes, *Atmos. Ocean, 17*, 77–92, 1979.

Negri, A.J., and R.F. Adler, Infrared and visible satellite rain estimation, 1, A grid cell approach, *J. Clim. Appl. Meteorol., 26*, 1553–1564, 1987a.

Negri, A.J., and R.F. Adler, Infrared and visible satellite rain estimation, 2, A cloud definition approach, *J. Clim. Appl. Meteorol., 26*, 1565–1576, 1987b.

Negri, A.J., R.F. Adler, and P.J. Wetzel, Satellite rain estimation: An analysis of the Griffith-Woodley technique, *J. Clim. Appl. Meteorol., 83*, 102–116. 1984.

Peck, E.L., Catchment modeling and initial parameter estimation for the National Weather Service Forecast system, *Rep. NWS HYDRO-31*, Natl. Oceanic and Atmos. Admin., Silver Spring, Md., 1976.

Rosenfeld, D., D. Atlas, and D.A. Short, The estimation of convective rainfall by area integrals, 2, Height-area rainfall threshold (HART) method, *J. Geophys. Res., 95*(D3), 2161–2176, 1990.

Scofield, R.A., and V.J. Oliver, A scheme for estimating convective rainfall from satellite imagery, *NOAA Tech. Memo. NESS 816*, 47 pp, Natl. Oceanic and Atmos. Admin., Silver Spring, Md., 1977.

Short, D.A., D.B. Wolff, D. Rosenfeld, and D. Atlas, A study of the threshold method utilizing raingauge data, *J. Appl. Meteor., 32*, 1279–1387, 1993.

Stout, J.E., D.W. Martin, and D.N. Sikdar, Estimating GATE rainfall with geosynchronous satellite images, *Mon. Weather Rev., 107*, 585–598, 1979.

Tsonis, A.A., On the separability of various classes from the GOES visible and infrared data, *J. Clim. Appl. Meteorol., 23*, 1393–1410, 1984.

Tsonis, A.A., and G.A. Isaac, On a new approach for instantaneous rain area delineation in the midlatitudes using GOES data, *J. Clim. Appl. Meteorol., 24*, 1208–1218, 1985.

Wallace, J. M., Diurnal variations in precipitation and thunderstorm frequency over the coterminous U.S., *Mon. Weather Rev., 103*, 406–419, 1975.

Winkler, J.A., B.R. Skeeter, and P.D. Yamamoto, Seasonal variations in the diurnal characteristics of heavy hourly precipitation across the United States, *Mon. Weather Rev., 116*, 1641–1658, 1988.

Wyss, J., E.R. Williams, and R.L. Bras, Hydrologic modeling of New England river basins using radar rainfall data, *J. Geophys. Res., 95*(D3), 2143–2152, 1990.

K.P.Georgakakos, Hydrologic Research Center, 12780 High Bluff Drive, Suite 260, San Diego, CA 92130.

G.N.Triantafyllou, Institute of Marine Biology of Crete, P.O.Box 2214, GR 71003 Iraklio, Crete, Greece. (e-mail: gt@imbc.gr)

A.A.Tsonis, University of Wisconsin–Milwaukee, Department of Geosciences, Lapham Hall, P.O.Box 413, Milwaukee, WI 53201. (e-mail: aatsonis@csd.uwm.edu)

(Received October 19, 1995; revised May 1, 1996;
accepted May 15, 1996.)